

Article

REE and Sr–Nd Isotope Characteristics of Cambrian–Ordovician Carbonate in Taebaek and Jeongseon Area, Korea

Tae-Hyeon Kim ^{1,2,*} , Seung-Gu Lee ¹  and Jae-Young Yu ²

¹ Geology Division, Korea Institute of Geoscience and Mineral Resources, Daejeon 34132, Korea; sgl@kigam.re.kr

² Division of Geology and Geophysics, Kangwon National University, Chuncheon 24341, Korea; jyu@kangwon.ac.kr

* Correspondence: chocochip222@naver.com; Tel.: +82-042-868-3969

Abstract: Carbonate formations of the Cambro-Ordovician Period occur in the Taebaek and Jeongseon areas, located in the central–eastern part of the Korean Peninsula. This study analyzed the rare earth element (REE) contents and Sr–Nd isotope ratios in these carbonates to elucidate their depositional environment and diagenetic history. The CI chondrite-normalized REE patterns of the carbonates showed negative Eu anomalies ($Eu_N / (Sm_N \times Gd_N)^{1/2} = 0.50$ to 0.81), but no Ce anomaly ($Ce/Ce^* = Ce_N / (La_N^2 \times Nd_N)^{1/3} = 1.01 \pm 0.06$). The plot of $\log(Ce/Ce^*)$ against sea water depth indicates that the carbonates were deposited in a shallow-marine environment such as a platform margin. The $^{87}Sr/^{86}Sr$ ratios in both Taebaek and Jeongseon carbonates were higher than those in the seawater at the corresponding geological time. The $^{87}Sr/^{86}Sr$ ratios and the values of $(La/Yb)_N$ and $(La/Sm)_N$ suggest that the carbonates in the areas experienced diagenetic processes several times. Their $^{143}Nd/^{144}Nd$ ratios varied from 0.511841 to 0.511980. The low ϵ_{Nd} values and high $^{87}Sr/^{86}Sr$ ratios in the carbonates may have resulted from the interaction with the hydrothermal fluid derived from the intrusive granite during the Cretaceous Period.

Keywords: carbonate; REE; Ce anomaly; Sr isotope; Nd isotope; carbonate depositional environment



check for updates

Citation: Kim, T.-H.; Lee, S.-G.;

Yu, J.-Y. REE and Sr–Nd

Isotope Characteristics of

Cambrian–Ordovician Carbonate in

Taebaek and Jeongseon Area, Korea.

Minerals **2021**, *11*, 326. [https://](https://doi.org/10.3390/min11030326)

doi.org/10.3390/min11030326

Academic Editor: Giovanni Mongelli

Received: 15 March 2021

Accepted: 19 March 2021

Published: 21 March 2021

Publisher's Note: MDPI stays neutral with regard to jurisdictional claims in published maps and institutional affiliations.



Copyright: © 2021 by the authors. Licensee MDPI, Basel, Switzerland. This article is an open access article distributed under the terms and conditions of the Creative Commons Attribution (CC BY) license (<https://creativecommons.org/licenses/by/4.0/>).

1. Introduction

The rare earth element (REE) patterns of carbonates can help understand their depositional environment and diagenetic processes [1–3]. Tanaka et al. [1] inferred the seawater depth of carbonate deposition according to the variation of Ce anomalies with the sea water depth. Madhavaraju et al. [2] deduced the paleo-redox condition changes from the Ce anomalies of the REE patterns of carbonates. In particular, the values of $(La/Yb)_N$ and Ce anomalies can be good indicators of the carbonate depositional environment [2,3]. Recently, Zhang et al. [3] reported that the REE pattern of a carbonate varies according to its tectonic setting. In addition, the $^{87}Sr/^{86}Sr$ ratios of carbonates are known to be insignificantly affected by the pore water during early diagenesis, but they can be raised by the interaction with hydrothermal fluid during a later diagenetic process [4–6]. The residence time of Nd in sea water is between 200 and 1000 years, while inter-ocean mixing requires about 1500 years [7]. For this reason, $^{143}Nd/^{144}Nd$ ratios in the Pacific, North Atlantic, and Indian oceans were all different despite the same geological time [8]. The $^{143}Nd/^{144}Nd$ ratio of carbonate has not yet been studied extensively, but recent studies showed a decrease in the $^{143}Nd/^{144}Nd$ ratio in carbonate during diagenesis. This is due to the diagenetic reaction with a fluid having lower $^{143}Nd/^{144}Nd$ than the carbonate [9,10].

Cambrian and Ordovician carbonate formations occur in the Taebaek and Jeongseon areas located in the central–eastern part of the Korean peninsula (Figure 1). These formations have been steadily investigated in various fields such as carbonate depositional

sedimentology [11–22], but their REE and Sr–Nd isotope geochemistry has not been investigated. Examining and interpreting the geochemical data from the carbonate rocks in the East Asian region may be the key to understanding the regional sedimentary environment and its evolution in the past. Fortunately, a considerable amount of geochemical work on the carbonate formations of the same geological time has been done in Japan and China; thus, it is necessary to examine the characteristics of the REE patterns and Sr–Nd isotope ratios of carbonate in the Korean peninsula. The aim of this study was to carry out a geochemical analysis of the carbonates in the study area and interpret their REE patterns and Sr–Nd isotope ratios to elucidate the depositional environments and diagenetic processes. The REE patterns and the isotopic ratios of the carbonates were also compared and discussed with those in Japan and China.

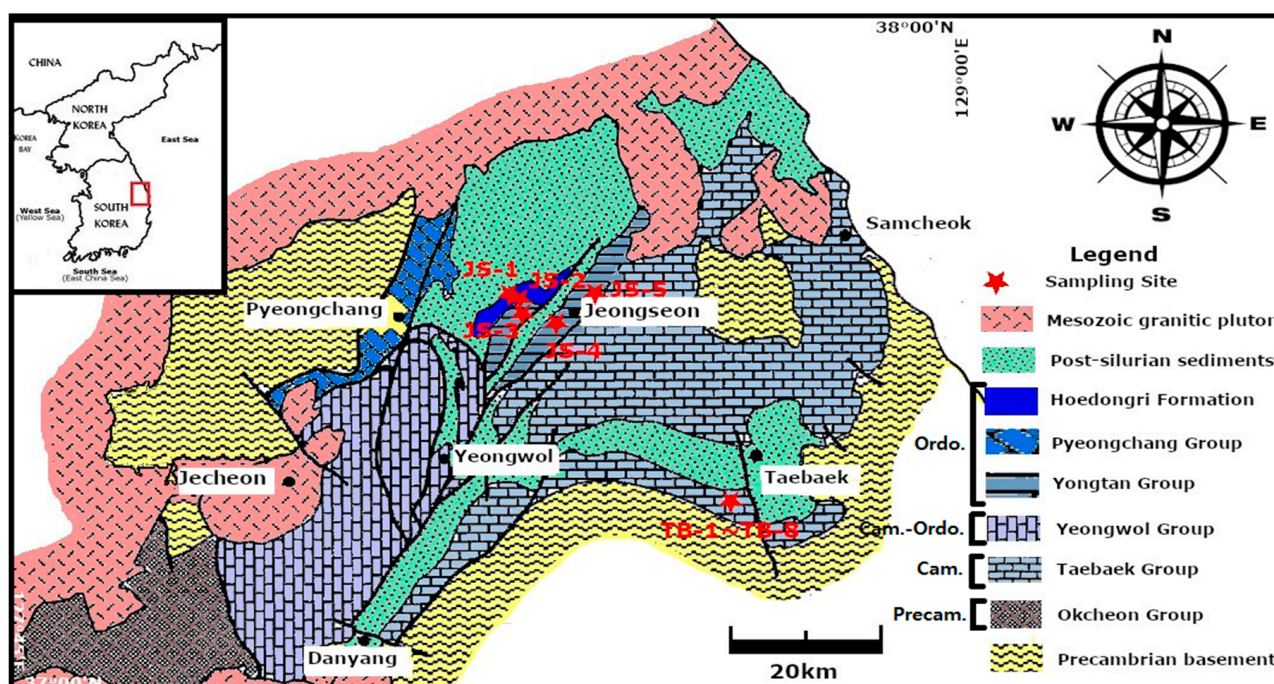


Figure 1. Geological map of Taebaek and Jeongseon areas, southeastern (SE) Korean Peninsula (modified from Kang and Choi [17]). Locations of samples are marked with a red star. Ordo, Cam, and Precam refer to Ordovician, Cambrian, and Precambrian, respectively.

2. Geological Background

2.1. Taebaek Area

The Cambrian carbonates in Taebaek area include the Myobong, Daegi, and Hwajeol Formations of the Taebaek group (Figure 1). Among these, the Daegi Formation mostly consists of carbonates, and it is widely distributed throughout the central–eastern part of the Korean Peninsula, including the Jeongseon, Samcheok, and Taebaek areas (Figure 1). The Daegi Formation is known to have been deposited in a shallow marine environment such as a platform margin [13,16,17]. Kim and Park [13] suggested that the Daegi Formation was deposited at a depth shallower than 10 m below sea level. Sim and Lee [16] studied the sequence stratigraphy of the Daegi Formation and concluded that the Daegi Formation experienced several sea-level fluctuations within the shallow depth range. A biostratigraphy and fossil study [17] also suggested that the Daegi Formation was formed in a shallow marine environment.

2.2. Jeongseon Area

The Jeongseon area, located northwest of Taebaek, consists of the Ordovician Yongtan and Cambrian Taebaek groups (Figure 1). The stratigraphy differs little from that of the

Taebaek area, except for the presence of the “Hoedongri” Formation. The “Hoedongri” Formation was named after the place where the conodont fossil thought to be of Silurian was first discovered [11]. Since then, many investigations have focused on the conodont fossil in the area to find out the geological age of these fossils and their stratigraphic significance [12,14,15]. Recently, Lee [18,19] insisted that the conodont fossils are not Silurian but Ordovician. Kwon et al. [20] discussed the evolution history of the Taebaek basin regarding the Hoedongri Formation as an Ordovician stratum. This study also regards the Hoedongri Formation as Ordovician. Won et al. [21] and Woo et al. [22] suggested that the carbonates in the area were deposited in a shallow marine environment. Most of the carbonates in the Jeongseon area have suffered recrystallization due to later metamorphism [12,14,15].

2.3. Petrography

The carbonates in the study areas consist of dark-gray to black fine-grained limestone and white crystalline limestone (Figure 2). They can be petrographically classified as well-sorted micrite to fine-grained calcite. The carbonates also include minor amounts of dolomite and illite. Figure 3 shows their microscope images. The carbonates in the study areas are mostly micrites that have been recrystallized (Figure 3A); however, some calcite crystals can be observed (Figure 3B). Therefore, identification of their origin using petrography is difficult. Although a little quartz was observed, this was negligible because there was almost no residue after acid digestion.

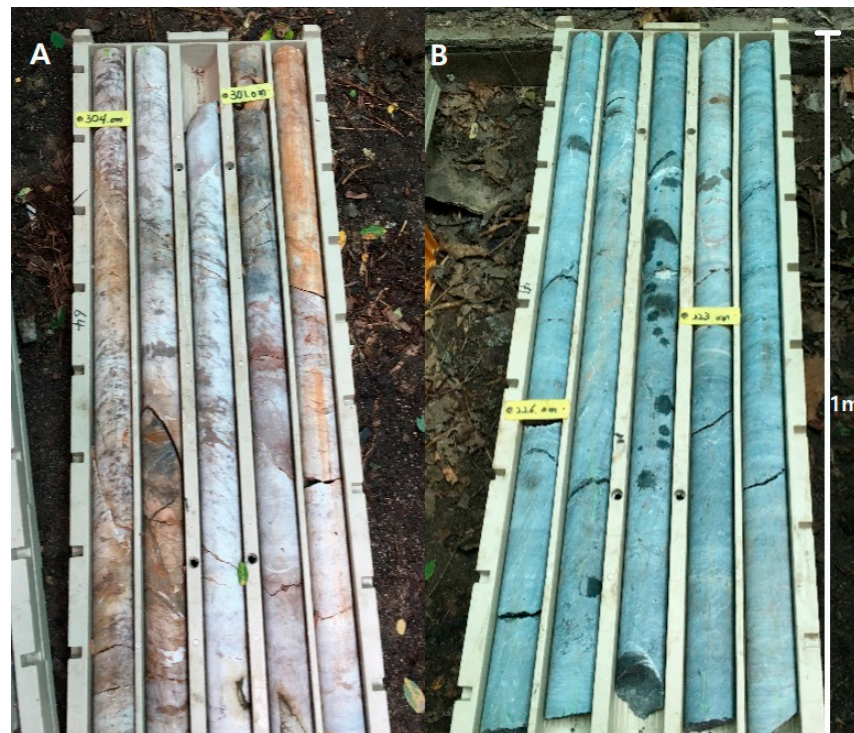


Figure 2. Carbonate samples in study area: (A) white crystalline limestone; (B) dark-gray fine-grained limestone.

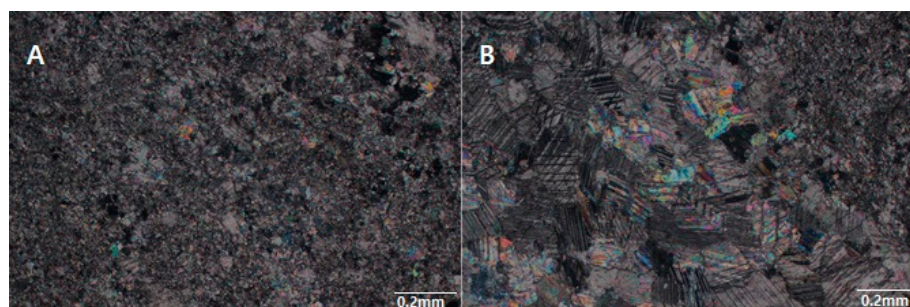


Figure 3. Microscope images of carbonate samples in study area: (A) recrystallized micrites; (B) micrites and calcites.

3. Methods

Thirteen carbonate samples were collected from five outcrops (samples JS-1 to JS-5) and eight drilling cores (samples TB-1 to TB-8). All the samples used were fresh and not very weathered. The samples were crushed using a jaw crusher and then pulverized in an agate mortar until their grain sizes were less than 150 μm . Ultra-pure HCl and HNO₃ reagents (Merck, Darmstadt, Germany) were used throughout sample preparation to minimize possible contamination from the reagents.

3.1. REE Analyses

For REE analyses, 0.5 to 1.0 g of the powdered samples were digested using 20 mL of 2 M HCl according to the method of Kim et al. [23], and then the digested sample solutions were filtered to remove the possible residue through the filter membrane having a 0.4 μm pore size. The silicate residues are known to have little effect on the solution chemistry [1,22]. Subsequently, the solutions were filtered using a 0.4 μm membrane filter and loaded into the cation-exchange resin (Bio-Rad, AG 50W-X8) column. The Ca matrix and Ba were removed by passing 2 M HCl and 2.4 M HNO₃ through the column, respectively. The REE fractions were recovered using 50 mL of 6 M HCl. The separated solutions were dried on a hot plate and diluted with 2% HNO₃ solution containing internal standards of In, Bi, and Re. The diluted REE solutions were analyzed using ICP-MS (Perkin Elmer, NexION350) at the Korea Institute of Geoscience and Mineral Resources (KIGAM). The sensitivity fluctuation of ICP-MS during the measurement was corrected from the internal standardization using In, Bi, and Re [24]. The levels of REE in the blank solutions were less than 10 ppt (10 $\mu\text{g/l}$). The accuracy and the precision of the analytical results were assessed with JDo-1 and JLS-1 carbonate reference materials curated by the Geological Survey of Japan (GSJ). The analysis results are reported with 95% confidence interval from the mean. The isobaric interferences were corrected by subtracting the signals of the corresponding oxides from each measurement. The oxides included ¹⁵¹Eu–¹³⁵Ba¹⁶O, ¹⁵⁹Tb–¹⁴³Nd¹⁶O, ¹⁶⁰Gd–¹⁴⁴Nd¹⁶O, ¹⁶⁵Ho–¹⁴⁹Sm¹⁶O, and others.

3.2. Sr and Nd Isotope Ratios

The sample digestion process for ⁸⁷Sr/⁸⁶Sr analysis was the same as that for REE analysis. The digested solutions were completely evaporated and then the residual cakes were dissolved again with 8 M HNO₃. The dissolved solutions were then loaded into the Sr-specific resin (SR-R50-S 50-100 mesh, Eichrom) and eluted with 8 M HNO₃ to collect elements other than Sr such as Rb, REE, and others. Lastly, Sr was separated from the resin with 0.05 M HNO₃ solution.

The other element fractions were dried up and loaded onto the cation-exchange resin (Bio-Rad, AG 50W-X8) column for REE separation. Nd was eluted from the separated REEs with 0.2 M 2-hydroxyisobutyric acid (HIBA) washed through a quartz column filled with the cation-exchange resin (Bio-Rad, AG 50W-X8, 200-400mesh).

The isotope composition of Sr and Nd was measured using a Neptune Plus MC-ICP-MS (Thermo Fisher Scientific Ltd.) with nine Faraday cups Neptune Plus, at KIGAM. The

analytical method of this study gave the $^{87}\text{Sr}/^{86}\text{Sr}$ of the NBS987 Sr standard as 0.710276 ± 0.000022 ($N = 20, 2\sigma_m$) and the $^{143}\text{Nd}/^{144}\text{Nd}$ of the JNdi-1 Nd standard as 0.512090 ± 0.000060 ($N = 20, 2\sigma_m$).

4. Results

4.1. REE Patterns

All the samples except JS-3 in the Taebaek and Jeongseon areas had relatively low REE concentrations ranging from 2.47 to 15.64 $\mu\text{g/g}$ (Table 1). The CI chondrite-normalized [25] REE patterns indicated that the carbonates were LREE enriched (Figure 4). The $(\text{La}/\text{Yb})_N$ values of the Taebaek and Jeongseon carbonates varied from 6.33 to 9.73 and 8.74 to 15.94, respectively. All REE patterns except that of JS-5, dolomite, showed negative Eu anomalies, but no Ce anomalies. The values of $\text{Eu}_N/(\text{Sm}_N \times \text{Gd}_N)^{1/2}$ in the carbonates ranged from 0.50 to 0.81. The average value of $\text{Ce}_N/(\text{La}_N^2 \times \text{Nd}_N)^{1/3}$ was 1.01 ± 0.06 . The REE pattern of JS-5 showed neither Ce nor Eu anomalies.

Table 1. Rare earth element (REE) contents of Taebaek and Jeongseon carbonates.

	La	Ce	Pr	Nd	Sm	Eu	Gd	Tb	Dy	Ho	Er	Tm	Yb	Lu	$(\text{La}/\text{Yb})_N^b$	Ce/Ce*	Eu/Eu*
TB-1	984 ^a	1835	226	884	191	46	191	29	185	40	118	17	106	16	6.33	0.96	0.74
TB-2	1821	3712	430	1694	353	70	336	57	339	68	184	25	159	24	7.78	1.00	0.62
TB-3	2417	4076	472	1771	378	72	360	57	342	69	195	27	174	27	9.43	0.90	0.60
TB-4	2708	5507	589	2294	463	107	420	64	389	76	214	30	194	27	9.47	1.03	0.74
TB-5	2744	5717	665	2567	542	108	508	79	488	102	274	42	256	36	7.27	1.03	0.63
TB-6	2732	5571	628	2442	478	80	422	71	441	87	240	35	208	31	8.91	1.02	0.54
TB-7	3003	6329	782	3204	668	178	666	96	547	99	263	38	230	34	8.88	0.99	0.81
TB-8	2607	4993	569	2210	424	93	399	59	333	67	191	29	182	28	9.73	0.97	0.69
JS-1	524	1053	122	441	78	16	71	11	62	12	32	5	28	4	12.30	1.02	0.65
JS-2	2801	6637	844	2927	553	90	550	83	499	91	251	36	222	32	8.74	1.12	0.51
JS-3	4434	9066	1117	4003	718	147	674	100	614	114	336	48	306	45	10.41	1.02	0.65
JS-4	1042	2138	244	1009	156	38	156	20	105	19	53	7	46	6	15.94	0.97	0.75
JS-5	1904	4544	593	2334	427	136	409	56	315	49	135	17	102	11	13.11	1.12	0.97

^a All units in ppb ($\mu\text{g}/\text{kg}$); ^b “_N” denotes the CI chondrite-normalized value. Ce/Ce* values are given according to $\text{Ce}_N/(\text{La}_N^2 \times \text{Nd}_N)^{1/3}$; Eu/Eu* values are given according to $\text{Eu}_N/(\text{Sm}_N \times \text{Gd}_N)^{1/2}$.

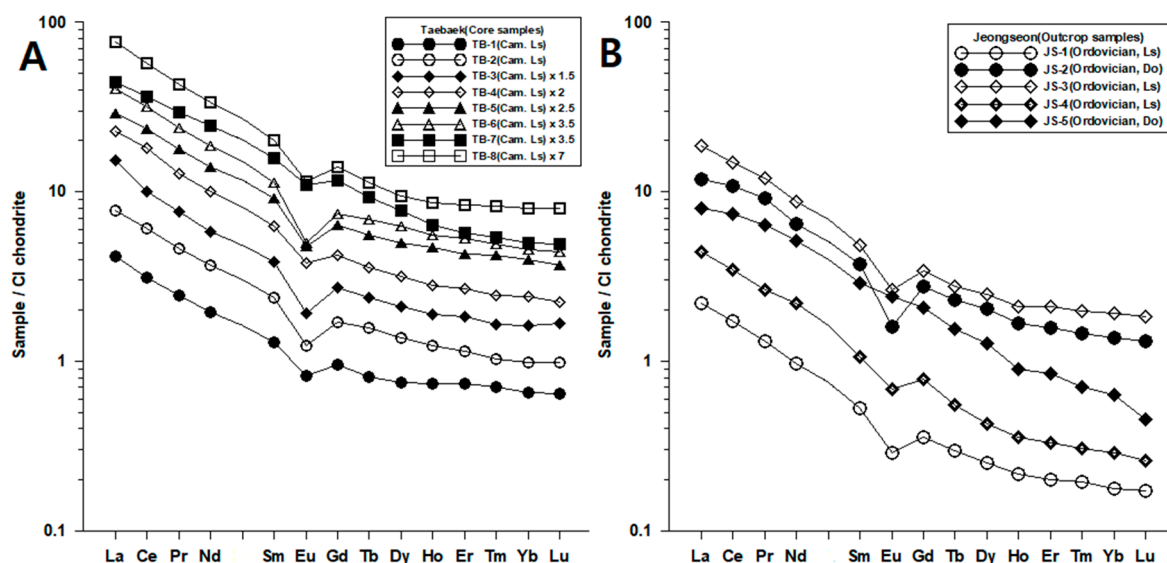


Figure 4. CI chondrite-normalized REE patterns of carbonates in Taebaek and Jeongseon. (A) CI chondrite-normalized REE patterns of Taebaek carbonates (core samples TB-1 to TB-8 collected at 173 m, 215 m, 226 m, 257 m, 287 m, 302 m, 331 m, and 353 m, respectively), (B) CI chondrite-normalized REE patterns of Jeongseon carbonates (outcrop samples JS-1 to JS-5). Cam. denotes Cambrian. Ls and Do denote limestone and dolomite, respectively. To improve visibility, the REE patterns of TB-3, 4, 5, 6, 7, and 8 were multiplied by 1.5, 2, 2.5, 3.5, 3.5, and 7, respectively.

4.2. $^{87}\text{Sr}/^{86}\text{Sr}$ and $^{143}\text{Nd}/^{144}\text{Nd}$ Ratios

The $^{87}\text{Sr}/^{86}\text{Sr}$ ratios of the Taebaek and Jeongseon carbonates varied from 0.70968 to 0.71116 and 0.70884 to 0.71114, respectively (Table 2, Figure 5). The average $^{87}\text{Sr}/^{86}\text{Sr}$ ratio of the Taebaek carbonates was 0.71013, which is a little higher than the average value 0.70975, of the Jeongseon carbonates. Sr concentrations of these samples ranged from 232 to 652 ppm, and there was no significant difference between the two areas. The $^{143}\text{Nd}/^{144}\text{Nd}$ ratios of the carbonates ranged from 0.511448 to 0.511980. Dolomite, TB-4, had the minimum value. Excluding dolomite, the range of $^{143}\text{Nd}/^{144}\text{Nd}$ ratio started from 0.511841. The ϵ_{Nd} values of the samples ranged from -23.2 to 12.8 . The ϵ_{Nd} value was calculated using the following equation:

$$\frac{(^{143}\text{Nd}/^{144}\text{Nd})_{\text{sample}} - (^{143}\text{Nd}/^{144}\text{Nd})_{\text{CHUR}}}{(^{143}\text{Nd}/^{144}\text{Nd})_{\text{CHUR}}} \times 10,000,$$

where the $(^{143}\text{Nd}/^{144}\text{Nd})_{\text{CHUR}}$ is given by 0.512638 [7].

Table 2. Sr and Nd isotope ratios of Taebaek and Jeongseon carbonates.

Sample Name	Sr (ppm)	$^{87}\text{Sr}/^{86}\text{Sr}$	$^{143}\text{Nd}/^{144}\text{Nd}$	$\epsilon_{\text{Nd}}(0)^a$
TB-1	278	0.709892	0.511970	-13.0
TB-2	258	0.709791	0.511870	-15.0
TB-3	234	0.709681	0.511886	-14.7
TB-4	270	0.710028	0.511448	-23.2
TB-5	304	0.710442	0.511900	-14.4
TB-6	246	0.711157	0.511960	-13.2
TB-7	299	0.709789	0.511851	-15.3
TB-8	321	0.710263	0.511841	-15.6
JS-1	306	0.708841	0.511895	-14.5
JS-2	266	0.709559	0.511980	-12.8
JS-3	652	0.710083	0.511856	-15.3
JS-4	358	0.709116	0.511881	-14.8
JS-5	232	0.711142	0.511940	-13.6

^a ϵ_{Nd} values are given according to $\epsilon_{\text{Nd}} = \{((^{143}\text{Nd}/^{144}\text{Nd})_{\text{sample}} - (^{143}\text{Nd}/^{144}\text{Nd})_{\text{CHUR}}) / (^{143}\text{Nd}/^{144}\text{Nd})_{\text{CHUR}}\} \times 10^4$; $(^{143}\text{Nd}/^{144}\text{Nd})_{\text{CHUR}} = 0.512638$.

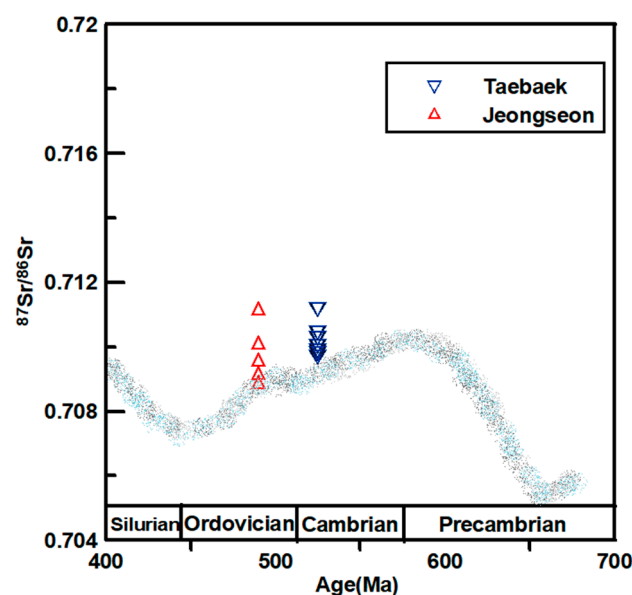


Figure 5. The $^{87}\text{Sr}/^{86}\text{Sr}$ ratios of the Taebaek and Jeongseon carbonates plotted as a $^{87}\text{Sr}/^{86}\text{Sr}$ variation diagram in Lower Paleozoic sea water (modified from Son and Kim [4]).

5. Discussion

5.1. Carbonate Depositional Environment

Carbonate is mostly deposited in shallow marine environments and, thus, its REE pattern reflects the characteristics of sea water at the time of its deposition [1–3]. Sea water usually shows REE patterns having negative Eu and Ce anomalies [26–30]. REEs generally have trivalent oxidation states in natural environments, but Ce can have a tetravalent state in oxidizing environments while Eu can have a divalent state in reducing environments [1–3]. Shallow marine environments can have fairly oxidizing conditions and precipitate CeO_2 , resulting in Ce deficiency and, consequently, negative Ce anomalies in the patterns in sea water [1–3]. Due to this redox behavior of Ce, the Ce anomalies in carbonate rocks are often used as an indicator of paleo-redox condition and the influence of terrigenous sediments [1–3]. Tanaka et al. [1] plotted the $\log(\text{Ce}/\text{Ce}^*)$ values of sea water against depth and showed that projecting the $\log(\text{Ce}/\text{Ce}^*)$ value of Japanese Permian carbonate using this plot can help understand the depositional environment of the carbonate.

Figure 6 shows the $\log(\text{Ce}/\text{Ce}^*)$ values of Taebaek and Jeongseon carbonates, ranging from -0.045 to -0.049 , displayed on a plot of $\log(\text{Ce}/\text{Ce}^*)$ of sea water vs. sea water depth. The plot suggests that the carbonates were deposited in shallow marine environments, which is consistent with the interpretation by previous sedimentary studies [13,16,17]. Limestone in the study areas shows a shallow marine environment facies including oolitic and bioclastic limestone [13,16], with a sedimentary structure indicating a shallow marine environment including a shallow upward structure [21,22]. It also contains many fossils indicating a shallow marine environment, such as trilobite and feeding traces [17,21]. Figure 6 matches well with the results of these sedimentary and biological studies. The REE patterns of marine carbonates generally have negative Ce anomalies; however, they may have little to no Ce anomalies because of carbonates mixing with the terrigenous clasts [2,3]. Carbonates in the study area showed no Ce anomalies, suggesting that they were deposited in a carbonate depositional environment, such as a platform margin, which can be easily affected by the terrigenous clasts.

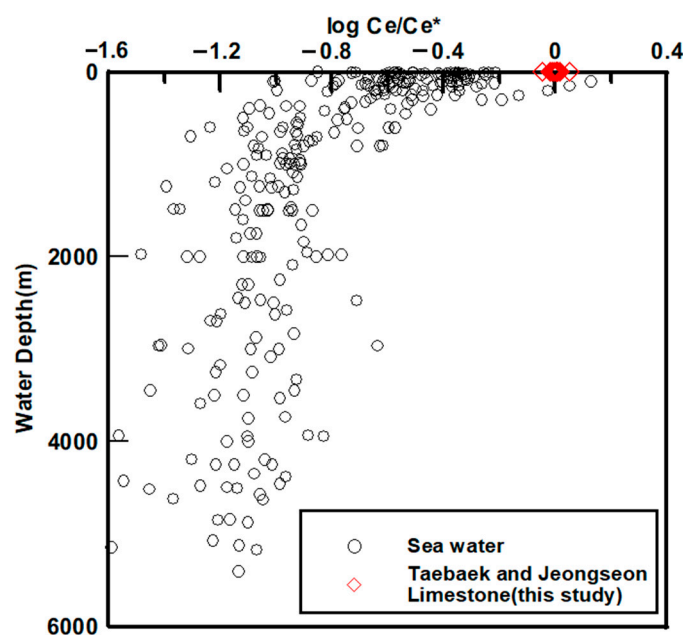


Figure 6. Plot of $\log(\text{Ce}/\text{Ce}^*)$ against the depth of sea water. The values of Taebaek and Jeongseon carbonates (marked red diamond) are plotted for comparison with seawater Ce anomalies. Here, $\log(\text{Ce}/\text{Ce}^*) = \log[\text{Ce}_N / (\text{La}_N^2 \times \text{Nd}_N)^{1/3}]$, where “N” denotes the CI chondrite-normalized value. REE values of seawater are quoted from German and Elderfield [26], Piepgras and Jacobsen [27], Bertram and Elderfield [28], Sholkovitz et al. [29], and German et al. [30].

5.2. Geochemical Significance of Sr and Nd Isotope Ratios in the Taebaek and Jeongseon Carbonates

Figure 5 shows the $^{87}\text{Sr}/^{86}\text{Sr}$ ratios of the Taebaek and Jeongseon carbonates plotted on the $^{87}\text{Sr}/^{86}\text{Sr}$ variation diagram of lower Paleozoic sea water, indicating that the carbonates from the study area had higher $^{87}\text{Sr}/^{86}\text{Sr}$ than those of Paleozoic seawater of the same age.

The higher $^{87}\text{Sr}/^{86}\text{Sr}$ ratios might be due to diagenesis [4–6,31–33]. The carbonate formations in the Korean peninsula experienced many diagenetic processes in the past [4,31–33], and the carbonates in the study area were recrystallized by hydrothermal water during the diagenesis [4,31–34]. Son and Kim [4] applied Banner's later diagenesis model (bulk recrystallization model) [5] to explain the higher $^{87}\text{Sr}/^{86}\text{Sr}$ ratio. They suggested that the higher $^{87}\text{Sr}/^{86}\text{Sr}$ ratio was caused by the Sr exchange between carbonate minerals and the hydrothermal fluid during the diagenetic recrystallization or refusion precipitation of the minerals [4,5]. The hydrothermal fluid which interacted with the host rock causing later diagenetic recrystallization generally had a high $^{87}\text{Sr}/^{86}\text{Sr}$ ratio [4–6]. Figure 7 shows the Sr concentration and $^{87}\text{Sr}/^{86}\text{Sr}$ change paths according to the two models of carbonate rock diagenetic processes by Banner [5]. The corresponding data of Taebaek and Jeongseon carbonates plotted on Figure 7 support the bulk recrystallization model.

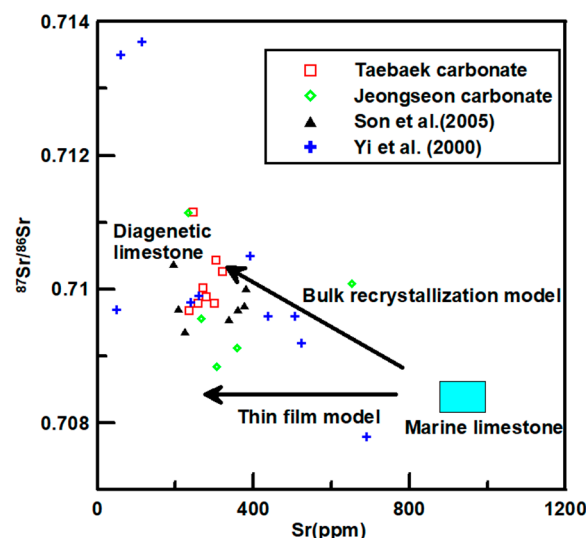


Figure 7. Banner's [5] later model of diagenesis processes in Paleozoic carbonate. Covariation in Sr isotopic composition and Sr concentration in Taebaek and Jeongseon carbonate.

Figure 8 shows the $(\text{La}/\text{Sm})_{\text{N}}$ and $(\text{La}/\text{Yb})_{\text{N}}$ values of the carbonates in the study area, normalized with Post Archean Australian Shale (PAAS [35]), on a scatter diagram with possible diagenetic pathways. Castorina et al. [10] reported that the $(\text{La}/\text{Yb})_{\text{N PAAS}}$ and $(\text{La}/\text{Sm})_{\text{N PAAS}}$ ratios can help distinguish various diagenetic processes on carbonates (Figure 8). The $(\text{La}/\text{Sm})_{\text{N PAAS}}$ values of the carbonate rocks fell within the specified range, but $(\text{La}/\text{Yb})_{\text{N PAAS}}$ values were relatively higher than the range of modern seawater. This indicates that the carbonates experienced early diagenesis. However, the $^{87}\text{Sr}/^{86}\text{Sr}$ ratio does not increase during the early diagenesis process, because the $^{87}\text{Sr}/^{86}\text{Sr}$ isotope ratio of the source that causes early diagenesis has a similar value to the $^{87}\text{Sr}/^{86}\text{Sr}$ isotope ratio of carbonate [5,6]. Thus, the carbonate rocks might have experienced a combination of early diagenesis processes to increase the $(\text{La}/\text{Sm})_{\text{N}}$ value and a later diagenesis process to increase the $^{87}\text{Sr}/^{86}\text{Sr}$ ratio.

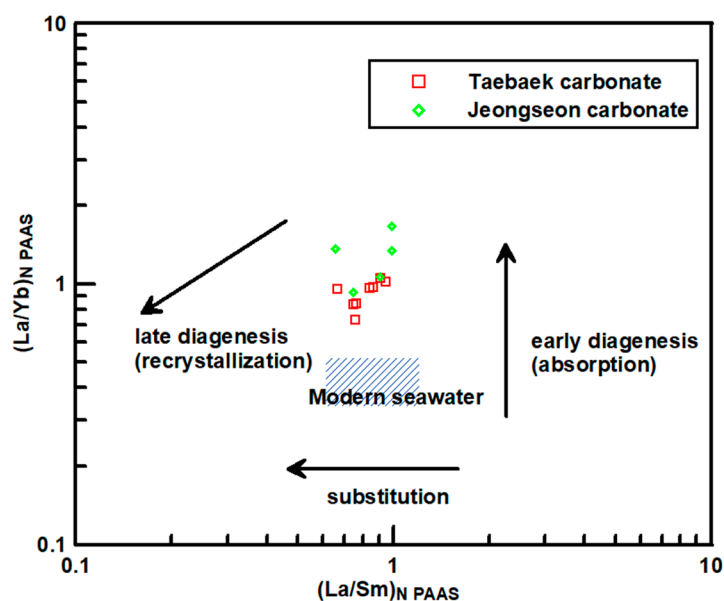


Figure 8. Covariation in $(\text{La}/\text{Sm})_{\text{N}}$ and $(\text{La}/\text{Yb})_{\text{N}}$ of Taebaek and Jeongseon carbonate. “n” denotes the PAAS (Post Archean Australian Shale, Taylor and McLennan [35])-normalized value. Modern seawater values are quoted from Garnit et al. [36] (modified from Castorina et al. [10]).

Figure 9 shows the covariation of $\epsilon_{\text{Nd}}(0)$ values and $^{87}\text{Sr}/^{86}\text{Sr}$ ratios of Taebaek and Jeongseon carbonates. The ϵ_{Nd} values used with $^{87}\text{Sr}/^{86}\text{Sr}$ can be very helpful to characterize the diagenetic processes. In Figure 9, the carbonates from the study area show relatively low $\epsilon_{\text{Nd}}(0)$ values compared to those of the common carbonates, ranging from 23.21 to -12.89 with an average value of -15.03 . Jakubowicz et al. [9] observed that the $\epsilon_{\text{Nd}}(0)$ and $^{87}\text{Sr}/^{86}\text{Sr}$ values in diagenetic seep carbonates tend to decrease and increase, respectively, as diagenesis progresses. As previously described, the $^{87}\text{Sr}/^{86}\text{Sr}$ ratio may be increased by interaction with the diagenetic source that causes the diagenetic process, such as hydrothermal fluid interacting with the host rock [4–6,31–33]. Although not much research has been done on the $\epsilon_{\text{Nd}}(0)$ with diagenesis of carbonate, this is also expected to result in lower $\epsilon_{\text{Nd}}(0)$ values of carbonate due to its interaction with a diagenetic source with lower $\epsilon_{\text{Nd}}(0)$ values than carbonate [9].

Figure 9 shows that the carbonates from the study area had higher $^{87}\text{Sr}/^{86}\text{Sr}$ and lower $\epsilon_{\text{Nd}}(0)$ values than those of Jakubowicz et al. [9]. $\epsilon_{\text{Nd}}(0)$ generally ranges from -3 to $+2$ in the Pacific Ocean [8], but these values were much lower in the carbonates from the study area. This decrease in $\epsilon_{\text{Nd}}(0)$ value is assumed to be due to the change during the diagenetic processes.

The sources of the hydrothermal fluid mediating the diagenesis of the carbonates in the study area have been disputed among the researchers [4,31–34]. Noh and Oh [31] determined K–Ar age and examined the chemistries of the carbonates in their study areas, and they concluded that the hydrothermal water originated from Mesozoic intrusive activities. Large Mesozoic granite bodies occur around the outskirts of the study area (Figure 1). Cheng and Chang [37] found that the ϵ_{Nd} and Sr isotopic compositions of the Mesozoic “Daebo” granite on the Korean Peninsula have the characteristics of a lower continental crust. Figure 8 shows that the $\epsilon_{\text{Nd}}(0)$ and $^{87}\text{Sr}/^{86}\text{Sr}$ values in the carbonates from the study area plotted fairly close to the range of Daebo granite. All these findings possibly support that the $^{143}\text{Nd}/^{144}\text{Nd}$ and $^{87}\text{Sr}/^{86}\text{Sr}$ ratios of the carbonates from the study area were modified by diagenetic processes mediated by the interactions with the hydrothermal fluids derived from Mesozoic intrusive bodies.

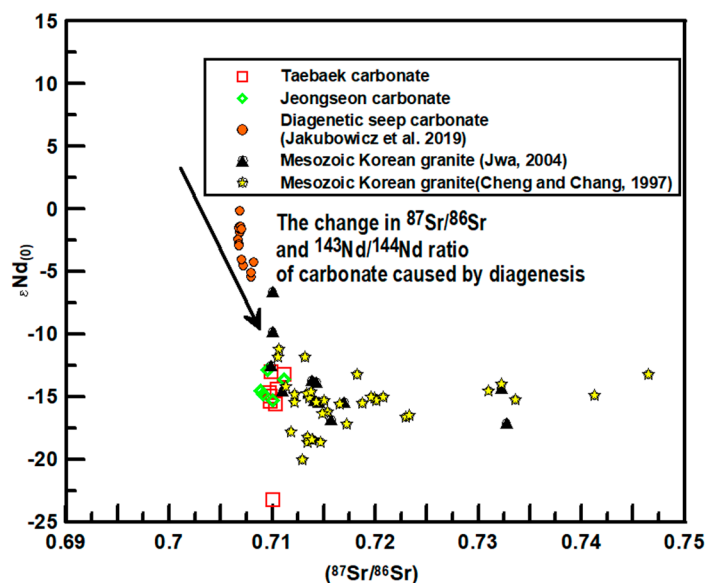


Figure 9. Covariation in $\epsilon_{Nd}(0)$ and $^{87}Sr/^{86}Sr$ of Taebaek (red rectangle) and Jeongseon (green diamond) carbonate. Mesozoic granite pluton of Korea (yellow star and black triangle) and diagenesis seep carbonate (orange circle) data quoted from Cheng and Chang [37], Jwa [38], and Jakubowicz et al. [9], respectively.

5.3. Comparison with the Carbonates in Japan and China

REE data of the carbonates in Japan and China have been extensively accumulated by many investigators [39–52]. Figures 10 and 11 show the CI chondrite-normalized REE patterns and Ce/Ce^* against $(La/Yb)_N$ plots of the carbonates in Japan and China, respectively.

Zhang et al. [3] recently reported the REE characteristics of the carbonates from various places around the world. The authors observed that the Ce anomalies and $(La/Yb)_N$ values of the carbonates varied depending on their depositional environments. The carbonates deposited under open sea environments have relatively low Ce/Ce^* and $(La/Yb)_N$ values, but those deposited under shallow marine environments have relatively high Ce/Ce^* and $(La/Yb)_N$ values [3]. This is because shallow marine environments have more terrigenous material input [3,53]. According to the observation of Zhang et al. [3], the Chinese carbonates were deposited in various environments (Figures 9 and 10). Their REE patterns, Ce anomalies, and $(La/Yb)_N$ values vary widely depending on the environments at the time of deposition [41,43–48,50–52]. The local redox condition should specifically affect Ce anomalies. Ling et al. [48] explained that the oxidizing condition due to oxygen supply to the shallow sea produced negative Ce anomalies in Chinese Ediacaran carbonate.

Extensive REE studies have been conducted on the Permian carbonates in Japan [2,39,40,42,49]. The Permian carbonates were mostly deposited in open sea environments such as an atoll. Figure 10 shows that the Permian carbonates have REE patterns with negative Ce anomalies and relatively low $(La/Yb)_N$ values. The average Ce anomalies and $(La/Yb)_N$ values of these carbonates are 0.38 and 7.21, respectively.

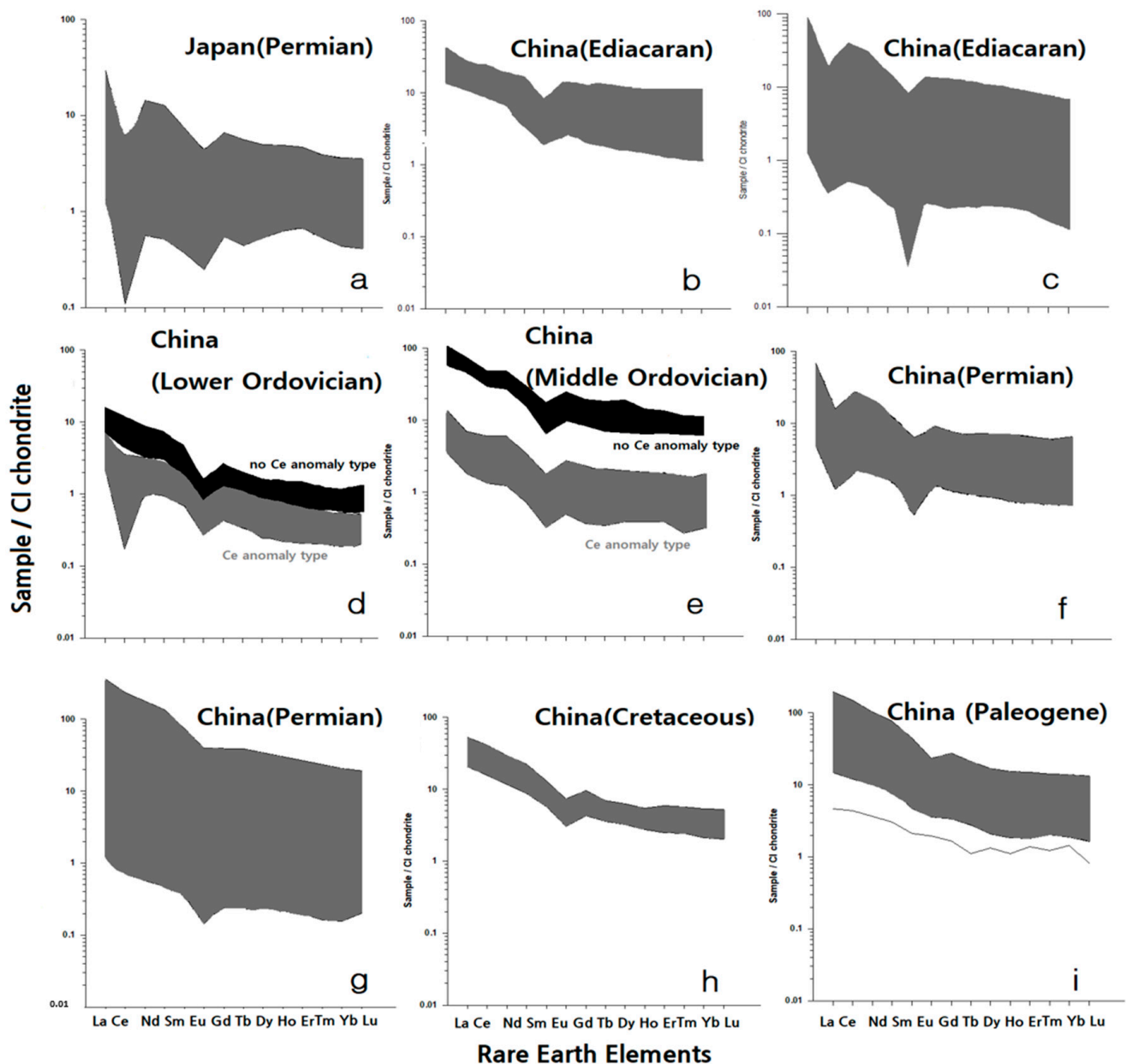


Figure 10. CI chondrite-normalized REE patterns of the carbonates in Japan and China. (a) Permian Japan carbonates, (b) Ediacaran (Type of disappear Ce anomaly), (c) Ediacaran China Carbonates (with Ce anomaly), (d) Lower Ordovician China Carbonates, (e) Middle Ordovician, (f) Permian China Carbonates (with Ce anomaly), (g) Permian China Carbonates (with no Ce anomaly), (h) Cretaceous China Carbonates, and (i) Paleogene China Carbonates. REE values are quoted from Kawabe et al. [39], Kunimaru et al. [40], Tanaka et al. [2], Bao et al. [41], Tanaka et al. [42], Zhang et al. [43], Zhao et al. [44], Jin et al. [45], Fu et al. [46], Qiu et al. [47], Ling et al. [48], Hori et al. [49], Zhang et al. [50], Yang et al. [51], and Su et al. [52].

The Cambrian–Ordovician carbonates of this study showed REE patterns with no Ce anomalies and high $(La/Yb)_N$ values. The average Ce anomalies and $(La/Yb)_N$ values in the Cambrian–Ordovician carbonates were 1.01 and 9.87, respectively. Figure 11 shows that the Korean carbonates plotted in the shallow marine area, while Japanese carbonates plotted in the open sea setting. This suggests that the Korean carbonates were deposited at places such as platform margins or inland, which are relatively more influenced by the influx of terrigenous material. At present, it may be difficult to understand the details of the past tectonic setting using carbonate geochemistry, but our results show the differences in the carbonate depositional environment among Korea, China, and Japan. Furthermore, a detailed study on platform margin carbonates, open sea carbonates, and various carbonate

depositional environments in Korea, Japan, and China is expected to clarify the depositional environment of the carbonates in East Asia.

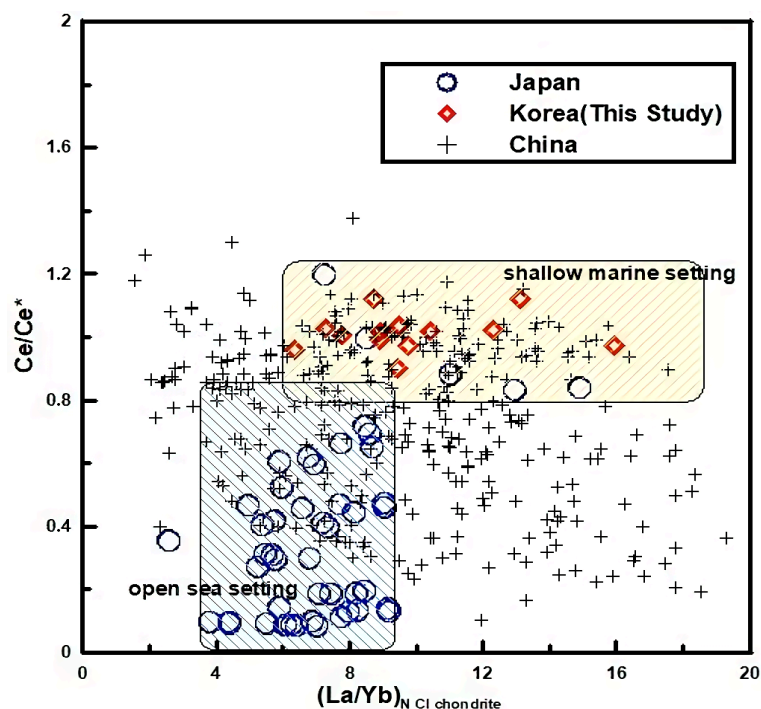


Figure 11. The plot of Ce/Ce^* against $(La/Yb)_N$ of the carbonates in Korea (red diamond), Japan (blue circle), and China (black cross). REE values of Japan and China carbonates are quoted from Kawabe et al. [39], Kunimaru et al. [40], Tanaka et al. [2], Bao et al. [41], Tanaka et al. [42], Zhang et al. [43], Zhao et al. [44], Jin et al. [45], Fu et al. [46], Qiu et al. [47], Ling et al. [48], Hori et al. [49], Zhang et al. [50], Yang et al. [51], and Su et al. [52]. The blue and yellow rectangles denote setting carbonates in an open sea depositional environment and a shallow marine depositional environment such as a platform margin, inland.

6. Conclusions

Cambrian and Ordovician carbonate formations occur in the Taebaek and Jeongseon areas located in the central–eastern part of the Korean peninsula. The REE patterns of the carbonates in the study area show negative Eu anomalies, but no Ce anomalies. This suggests that the carbonates in the Taebaek and Jeongseon areas were deposited in a shallow marine environment such as a platform margin, which can be significantly influenced by the terrigenous material input. $^{87}Sr/^{86}Sr$ ratios of the carbonates in the study area are higher than that of seawater, suggesting an interaction between the carbonates and hydrothermal fluid during the late diagenetic process. Subsequently, the $(La/Sm)_N$ and $(La/Yb)_N$ ratios of carbonates in study area suggest that the carbonates had experienced an early diagenetic process (possibly mediated by pore water). Therefore, carbonates in the study area are estimated to have experienced a combination of early and late diagenesis. High $^{87}Sr/^{86}Sr$ and low $^{143}Nd/^{144}Nd$ values suggest that the main source of the fluid resulting in the late diagenesis of Taebaek and Jeongseon carbonates was hydrothermal fluid from the “Daebo” intrusive granite around the outskirts of the study area. Carbonates in the study area show high $(La/Yb)_N$ values and no Ce anomalies. This indicates that the carbonates in the study area were deposited in an environment different from those of Japan and China, nearby East Asian countries. These geochemical characteristics are expected to help identify the carbonate depositional environments in East Asian countries and provide an in-depth understanding of their depositional processes.

Author Contributions: Conceptualization and methodology, S.-G.L. and T.-H.K.; investigation, T.-H.K.; writing—original draft preparation, T.-H.K.; writing—review and editing, J.-Y.Y. and S.-G.L.; funding acquisition, KIGAM. All authors read and agreed to the published version of the manuscript.

Funding: This research was supported by the Basic Research Project of the Korea Institute of Geoscience and Mineral Resources (KIGAM), funded by the Ministry of Science and ICT (GP2020-003).

Acknowledgments: The authors thank the two anonymous reviewers for their helpful and constructive reviews of the manuscript.

Conflicts of Interest: The authors declare no conflict of interest.

References

1. Tanaka, K.; Miura, N.; Asahara, Y.; Kawabe, I. Rare earth element and strontium isotopic study of seamount-type carbonates in Mesozoic accretionary complex of Southern Chichibu Terrane, central Japan: Implication for incorporation process of seawater REE into carbonates. *Geochem. J.* **2003**, *37*, 163–180. [[CrossRef](#)]
2. Madhavaraju, J.; Loser, H.; Lee, Y.-I.; Santacruz, L.R.; Pi-Puig, T. Geochemistry of Lower Cretaceous carbonates of the Alisitos Formation, Baja California, Mexico: Implications for REE source and paleo-redox conditions. *J. S. Am. Earth Sci.* **2016**, *66*, 149–165. [[CrossRef](#)]
3. Zhang, K.J.; Li, Q.H.; Yan, L.L.; Zeng, L.; Lu, L.; Zhang, Y.X.; Hui, J.; Jin, X.; Tang, X.C. Geochemistry of carbonate deposited in various plate tectonic settings. *Earth Sci. Rev.* **2017**, *167*, 27–46. [[CrossRef](#)]
4. Son, J.H.; Kim, G.H. Geochemical and Strontium Isotopic Compositions for Carbonate Rocks from the Hoedongri Formation in the Jeongseon Area, South Korea. Master's Thesis, Ewha University, Seoul, Korea, 2005.
5. Banner, J.L. Application of the trace element and isotope geochemistry of strontium to studies of carbonate diagenesis. *Sedimentology* **1995**, *42*, 805–824. [[CrossRef](#)]
6. Clauer, N.; Chaudhuri, S.; Subramaniam, R. Strontium isotopes as indicators of diagenetic recrystallization scales within carbonate rocks. *Chem. Geol. Isot. Geosci. Sect.* **1989**, *80*, 27–34. [[CrossRef](#)]
7. Huh, Y.; Jang, K. Authigenic Neodymium Isotope Record of Past Ocean Circulation. *J. Petrol. Soc. Korea* **2014**, *23*, 249–259. [[CrossRef](#)]
8. Piepgras, D.J.; Wasserburg, G.J. Neodymium Isotopic Variations in Seawater. *Earth Planet. Sci. Lett.* **1980**, *50*, 128–138. [[CrossRef](#)]
9. Jakubowicz, M.; Dopieralska, J.; Kaim, A.; Skupien, P.; Kiel, S.; Belka, Z. Nd isotope composition of seep carbonates: Towards a new approach for constraining seafloor fluid circulation at hydrocarbon seeps. *Chem. Geol.* **2019**, *503*, 40–51. [[CrossRef](#)]
10. Castornia, F.; Masi, U.; Billi, A. Assessing the origin of Sr and Nd isotopes and (REE + Y) in Middle-Upper Pleistocene travertines from the Acquasanta Terme area (Marche, central Italy) and implications for neotectonics. *Appl. Geochem.* **2020**, *117*, 104596. [[CrossRef](#)]
11. Lee, H.Y. Conodont Fauna from the Great Carbonate Series in Dongjeom District, Samcheong-Gun, Gangweon-Do and its Stratigraphical Significance. *J. Geol. Soc. Korea* **1971**, *7*, 89–101.
12. Lee, H.Y. A Study on Biostratigraphy and Bioprovince of the Middle Ordovician Conodonts from South Korea: With special reference to the Conodonts from Yeongheung Formation. *J. Geol. Soc. Korea* **1979**, *15*, 37–60.
13. Kim, J.Y.; Park, Y.A. Sedimentological Study on the Pungchon and Hwajol Formations, Gangweondo, Korea. *J. Geol. Soc. Korea* **1981**, *17*, 225–240.
14. Lee, B.-S.; Choi, D.-K.; Lee, H.Y. Conodonts from the Machari Formation (Middle?-Upper Cambrian) in the Yeongweol Area, Kangweon-do, Korea. *J. Geol. Soc. Korea* **1991**, *27*, 394–408.
15. Seo, K.-S.; Lee, H.-Y.; Moon, H.-S.; Song, Y.G. Mineral Chemistry of Biogenic Apatite in Lower Ordovician Conodont and Its Potential and Limitation for Stratigraphical Implication. *J. Geol. Soc. Korea* **1991**, *27*, 259–270.
16. Sim, M.-S.; Lee, Y.-I. Sequence stratigraphy of the Middle Cambrian Daegi Formation (Korea), and its bearing on the regional stratigraphic correlation. *Sediment. Geol.* **2006**, *191*, 151–169. [[CrossRef](#)]
17. Kang, I.-S.; Choi, D.-K. Middle Cambrian trilobites and biostratigraphy of the Daegi Formation (Taebaek Group) in the Seokgaejae section, Taebaeksan Basin, Korea. *Geosci. J.* **2007**, *11*, 279–296. [[CrossRef](#)]
18. Lee, B.-S. Recognition and significance of the *Aurilobodus serratus* Conodont Zone (Darriwilian) in lower Paleozoic sequence of the Jeongseon—Pyeongchang area, Korea. *Geosci. J.* **2018**, *22*, 683–696. [[CrossRef](#)]
19. Lee, B.-S. Upper Ordovician (Sandbian) conodonts from the Hoedongri Formation of western Jeongseon, Korea. *Geosci. J.* **2019**, *23*, 695–705. [[CrossRef](#)]
20. Kwon, Y.-K.; Kwon, Y.-J.; Yeo, J.-M.; Lee, C.-Y. Basin Evolution of the Taebaeksan Basin during the Early Paleozoic. *Econ. Environ. Geol.* **2019**, *52*, 427–448.
21. Won, J.-H.; Lee, H.-Y.; Woo, K.-S. Sedimentological study on the Jeongseon Carbonate Pyeongchang Group and Yongtan Group, Kangwon-Do, Korea. In Proceedings of the Geological Society of Korea, Jeju, Korea, 28–31 October 2015; p. 272.
22. Woo, K.-S.; Ju, S.-O. Stratigraphic and sedimentological meaning of the Yongtan Group (Joseon Supergroup), Korea. In Proceedings of the Geological Society of Korea, Pyeongchang, Korea, 26–29 October 2016; p. 98.

23. Kim, T.-H.; Lee, S.-G.; Yu, J.-Y.; Tanaka, T. Study on REE Analysis of Carbonate: Effect of Ba Oxide and Hydroxide Interferences on ICP-MS REE Analysis for Geological Samples. *J. Geol. Soc. Korea* **2019**, *55*, 759–770. [[CrossRef](#)]
24. Kim, T.-H.; Tanaka, T.; Lee, S.-G.; Han, S.; Yoo, I.-S.; Park, S.-B.; Lee, J.-I. Quantitative analysis of REEs in geological samples using ICP-MS: Effect of oxide and hydroxide interference on REEs. In Proceedings of the 28th Proceedings Annual Joint Conference the Petrological Society of Korea and Mineralogical Society of Korea, Busan, Korea, 29–30 May 2014; pp. 29–30.
25. McDonough, W.F.; Sun, S.S. The Composition of the Earth. *Chem. Geol.* **1995**, *120*, 223–253. [[CrossRef](#)]
26. German, C.R.; Elderfield, H. Rare earth elements in the NW Indian Ocean. *Geochim. Cosmochim. Acta* **1990**, *54*, 1929–1940. [[CrossRef](#)]
27. Piepgras, D.J.; Jacobsen, S.B. The behavior of rare earth elements in seawater: Precise determination of variations in the North Pacific water column. *Geochim. Cosmochim. Acta* **1992**, *56*, 1851–1862. [[CrossRef](#)]
28. Bertram, C.J.; Elderfield, H. The geochemical balance of the rare earth elements and neodymium isotopes in the oceans. *Geochim. Cosmochim. Acta* **1993**, *57*, 1957–1986. [[CrossRef](#)]
29. Sholkovitz, E.R.; Landing, W.M.; Lewis, B.L. Ocean particle chemistry: The fractionation of rare earth elements between suspended particles and seawater. *Geochim. Cosmochim. Acta* **1994**, *58*, 1567–1579. [[CrossRef](#)]
30. German, C.R.; Masuzawa, T.; Greaves, M.J.; Elderfield, H.; Edmond, J.M. Dissolved rare earth elements in the Southern Ocean: Cerium oxidation and the influence of hydrography. *Geochim. Cosmochim. Acta* **1995**, *59*, 1551–1558. [[CrossRef](#)]
31. Noh, J.H.; Oh, S.J. Hydrothermal Alteration of the Pungcheon Carbonate and the Formation of High-Ca Carbonate. *J. Geol. Soc. Korea* **2005**, *41*, 175–197.
32. Yoon, K.H.; Woo, K.S. Textural and geochemical characteristics of crystalline carbonate (high-purity carbonate) in the Daegi Formation, Korea. *J. Geol. Soc. Korea* **2006**, *42*, 561–576.
33. Kim, C.S.; Choi, S.-G.; Kim, G.-B.; Kang, J.; Kim, K.B.; Kim, H.; Lee, J.; Ryu, I. Genetic Environments of the High-purity Carbonate in the Upper Zone of the Daegi Formation at the Jeongseon-Samcheok Area. *Econ. Environ. Geol.* **2017**, *50*, 287–302.
34. Yi, J.-M.; Kim, K.H.; Tanaka, T.; Kawabe, I. REE and Sr isotopic compositions of carbonate pebbles in the phyllitic rocks of the Hwanggangni Formation, Okcheon zone. *J. Geol. Soc. Korea* **2000**, *36*, 257–278.
35. Taylor, S.R.; McLennan, S.M. *The Continental Crust: Its Composition and Evolution*; Blackwell: Oxford, UK, 1985.
36. Garnit, H.; Bouhlef, S.; Barca, D.; Chtara, C. Application of LA-ICP-MS to sedimentary phosphatic particles from Tunisian phosphorite deposits: Insights from trace elements and REE into paleo-depositional environments. *Geochemistry* **2012**, *72*, 127–139. [[CrossRef](#)]
37. Cheong, C.-S.; Chang, H.-W. Sr, Nd, and Pb isotope systematics of granitic rocks in the central Ogcheon Belt, Korea. *Geochem. J.* **1997**, *31*, 17–36. [[CrossRef](#)]
38. Jwa, Y.-J. Possible source rocks of Mesozoic granite in South Korea: Implications for crustal evolution in NE Asia. *Earth Environ. Sci. Trans. R. Soc. Edinb.* **2004**, *95*, 181–198.
39. Kawabe, I.; Inoue, T.; Kitamura, S. Comparison of REE analyses of GSF carbonate reference rocks by ICP-AES and INAA: Fission and spectral interferences in INAA determination of REE in geochemical samples with high U/REE ratios. *Geochem. J.* **1994**, *28*, 19–29. [[CrossRef](#)]
40. Kunimaru, T.; Shimizu, H.; Takahashi, K.; Yabuki, S. Differences in geochemical features between Permian and Triassic cherts from the Southern Chichibu terrane, southwest Japan: REE abundances, major element compositions and Sr isotopic ratio. *Sediment. Geol.* **1998**, *119*, 195–217. [[CrossRef](#)]
41. Bao, Z.; Zhao, Z.; Guha, J.; Williams-Jones, A.E. HFSE, REE, and PGE geochemistry of three sedimentary rock-hosted disseminated gold deposits in southwestern Guizhou Province, China. *Geochem. J.* **2004**, *38*, 363–381. [[CrossRef](#)]
42. Tanaka, K.; Kawabe, I. REE abundance in ancient seawater inferred from marine carbonate experimental REE partition coefficients between calcite and aqueous solution. *Geochem. J.* **2006**, *40*, 425–435. [[CrossRef](#)]
43. Zhang, X.; Hu, W.; Jin, Z.; Zhang, J. REE Composition of Lower Ordovician Dolomites in Central and North Tarim Basin, NW China: A Potential REE Proxy for Ancient Seawater. *Acta Geol. Sin. Engl. Ed.* **2008**, *82*, 610–621.
44. Zhao, Y.-Y.; Zheng, Y.-F.; Chen, F. Trace element and strontium isotope constraints on sedimentary environment of Ediacaran carbonates in southern Anhui, South China. *Chem. Geol.* **2009**, *265*, 345–362. [[CrossRef](#)]
45. Jin, Z.; Zhu, D.; Hu, W.; Zhang, X.; Zhang, J.; Song, Y. Mesogenetic dissolution of the middle Ordovician carbonate in the Tahe oilfield of Tarim basin, NW China. *Mar. Pet. Geol.* **2009**, *26*, 753–763. [[CrossRef](#)]
46. Fu, X.; Wang, J.; Zeng, Y.; Tan, F.; Feng, X. REE geochemistry of marine oil shale from the Changshe Mountain area, Northern Tibet, China. *Int. J. Coal Geol.* **2010**, *81*, 191–199. [[CrossRef](#)]
47. Qiu, Z.; Wang, Q.; Yan, D. Geochemistry of the Middle to Late Permian carbonates from the marginal zone of an isolated platform (Laibin, South China). *Sci. China Earth Sci.* **2013**, *56*, 1688–1700. [[CrossRef](#)]
48. Ling, H.-F.; Chen, X.; Li, D.; Wang, D.; Shields-Zhou, G.A.; Zhu, M. Cerium anomaly variations in Ediacaran-earliest Cambrian carbonates from the Yangtze Gorges area, South China: Implications for oxygenation of coeval shallow seawater. *Precambrian Res.* **2013**, *225*, 110–127. [[CrossRef](#)]
49. Hori, M.; Ishikawa, T.; Nagaishi, K.; You, C.-F.; Huang, K.-F.; Shen, C.-C.; Kano, A. Rare earth elements in a stalagmite from southwestern Japan: A potential proxy for chemical weathering. *Geochem. J.* **2014**, *48*, 73–84. [[CrossRef](#)]
50. Zhang, P.; Hua, H.; Liu, W. Isotopic and REE evidence for the paleoenvironmental evolution of the late Ediacaran Dengying Section, Ningqing of Shaanxi Province, China. *Precambrian Res.* **2014**, *242*, 96–111. [[CrossRef](#)]

51. Yang, Y.; Gao, F.; Chen, C.; Pu, X. A Transgressive Depositional Setting for the Paleogene Shahejie Formation in the Qikou Depression, Eastern China: Inferences from the REE Geochemistry of Carbonates. *J. Earth Sci.* **2018**, *29*, 326–341. [[CrossRef](#)]
52. Su, C.; Li, F.; Tan, X.; Gong, Q.; Zeng, K.; Tang, H.; Li, M.; Wang, X. Recognition of diagenetic contribution to the formation of carbonate-marl alternations: A case study from Permian of south China. *Mar. Pet. Geol.* **2019**, in press.
53. Tostevin, R.; Wood, R.A.; Shields, G.A.; Poulton, S.W.; Guilbaud, R.; Bowyer, F.; Penny, A.M.; He, T.; Curtis, A.; Hoffmann, K.H.; et al. Low-oxygen waters limited habitable space for early animals. *Nat. Commun.* **2016**, *7*, 1–9. [[CrossRef](#)]